Journal of Crystal Growth 98 (1989) 209–219
North-Holland, Amsterdam

EFFECTS OF AlN BUFFER LAYER ON CRYSTALLOGRAPHIC STRUCTURE AND ON ELECTRICAL AND OPTICAL PROPERTIES OF GaN AND $Ga_{1-x}Al_xN$ ($0 < x \leqq 0.4$) FILMS GROWN ON SAPPHIRE SUBSTRATE BY MOVPE

Isamu AKASAKI, Hiroshi AMANO, Yasuo KOIDE, Kazumasa HIRAMATSU and Nobuhiko SAWAKI

Nagoya University, Department of Electronics, Furo-cho, Nagoya 464-01, Japan

GaN and $Ga_{1-x}Al_xN$ ($0 < x \leqq 0.4$) films grown by MOVPE on (0001) sapphire substrate are found to consist of many mosaic crystallites with various orientations. By preceding deposition of a thin AlN buffer layer, the microscopic fluctuation in crystallite orientation can be considerably reduced and the crystalline quality of the film is remarkably improved. Both the thickness and the deposition temperature of the AlN layer are found to be optimal as a buffer layer to convey the information of the substrate such as the crystallographic orientation and to relax the strain in this heteroepitaxial growth. The essential role of the AlN buffer layer is thought to be the supply of nucleation centers having the same orientation as the substrate and the promotion of lateral growth of the film due to the decrease in interfacial free energy between the film and the substrate.

1. Introduction

Gallium nitride (GaN) and gallium aluminum nitride ($Ga_{1-x}Al_xN$) alloy are promising materials for optical devices in the blue and UV regions, since they have direct band gaps wider than 3.4 eV and electrical resistivities over a wide range from 10^{-4} up to 10^{8} Ω cm at room temperature [1,2].

Various methods have been reported on the growth of single crystal films of these materials. They include hydride vapor phase epitaxy (HVPE), MBE and MOVPE using a sapphire single crystal as the substrate.

In contrast to other III–V compound semiconductors such as GaAs and InP, however, it has been difficult to grow high quality epitaxial films, especially with a smooth surface free from cracks, because of the large lattice mismatch and the large difference in the thermal expansion coefficient between the nitride film and the sapphire substrate, as shown in table 1.

Recently, we succeeded in improving remarkably the surface morphology as well as the electrical and optical properties of GaN and $Ga_{1-x}Al_xN$ ($0 < x \leqq 0.4$) alloy films by the preceding deposition of a thin AlN layer as a buffer layer before

Table 1
Lattice and thermal mismatches between nitride and sapphire

		Lattice constant (Å)	$\Delta a_{epi}/\Delta a_{sub}$ (%)	Thermal expansion coefficient $\times 10^{-6}$ (K^{-1})	$\Delta\alpha_{epi}/\Delta\alpha_{sub}$ (%)
GaN	a	3.189	+16.1	5.59	−25.5
	c	5.182	–	7.75	−8.8
AlN	a	3.111	+13.2	5.3	−29.3
	c	4.980	–	4.2	−50.6
Sapphire	a	4.758	–	7.5	–
	c	12.991	–	8.5	–

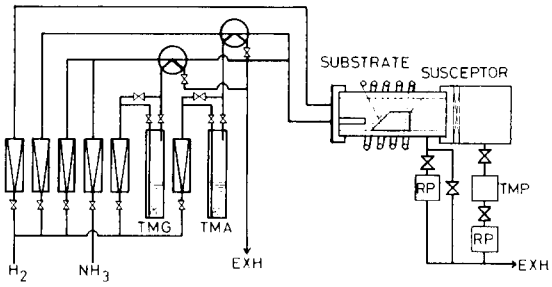

Fig. 1. Schematic drawing of growth apparatus.

GaN (or the alloy) film growth by MOVPE [3,4].

In this paper, the effects of the AlN buffer layer on the crystallographic structure and the electrical and optical properties of GaN and the alloy films will be discussed.

2. Experimental

A horizontal type MOVPE reactor operated at atmospheric pressure was used for the growth. Trimethylgallium (TMG), trimethylaluminum (TMA) and ammonia (NH_3) were used as source materials. The carrier gas was hydrogen (H_2). In order to reduce parasitic reactions of metalorganics (MO) with NH_3, H_2 carrier gas, MO and NH_3 were mixed just before the reactor, and the mixture was fed to a slanted substrate through a delivery tube with a high velocity (110 cm/s) as shown in fig. 1. Thus, the desired alloy composition over the whole range was obtained by controlling the concentration ratio of TMG to TMA [5].

Optical grade polished sapphire with (0001) orientation (C-face) was used as the substrate. The misorientation was within $\pm 0.5°$. The substrate was etched with a hot solution of $H_3PO_4 : H_2SO_4 = 1 : 3$ and placed on a graphite susceptor which was heated by RF. Prior to the epitaxial growth, it was thermally treated at 1150 °C for 10 min in a stream of H_2 to remove surface damage.

Conventionally, GaN or the alloy film is grown directly on the substrate, as shown in fig. 2b. In a newly developed process, shown in fig. 2a, before the growth of GaN or the alloy film, a thin AlN layer of about 500 Å thick was deposited at 600 °C for 6 min by feeding 7 μmol/min of TMA and 2 SLM of NH_3 diluted with 2.5 SLM of H_2. Then, the substrate temperature was raised to a growth temperature of 1000 °C, so that a GaN (or the alloy) film of about 3–12 μm thick was grown in the same way as the conventional process. Fig. 2c shows the timing chart of the growth process. Under these conditions, single crystal films of

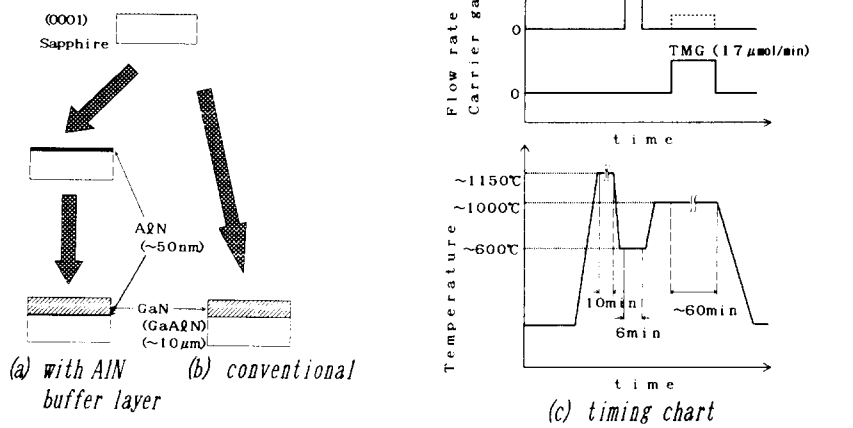

Fig. 2. Illustration of growth process: (a) with the AlN buffer layer and (b) conventional; (c) shows the timing chart.

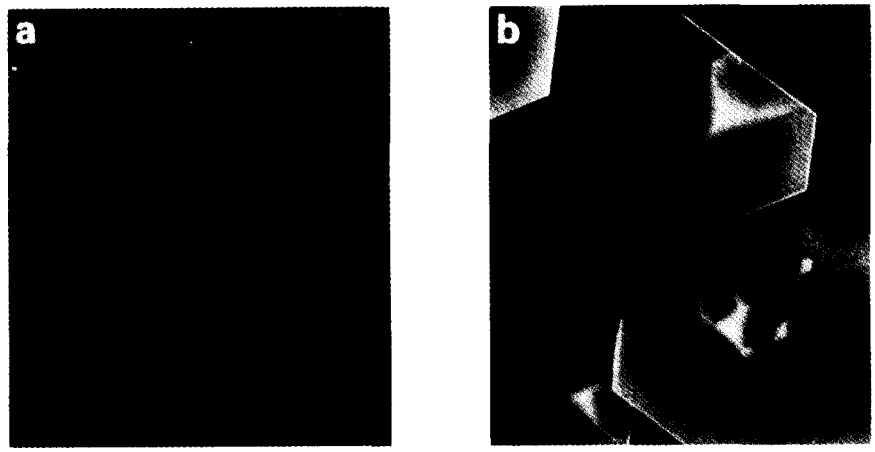

Fig. 3. SEM photographs of GaN film grown on (0001) sapphire (a) with (500 Å thick) and (b) without AlN buffer layer. The growth time was 60 min. Markers represent 1 μm.

GaN and $Ga_{1-x}Al_xN$ alloys with AlN molar fraction x smaller than 0.4 can be grown. Single crystal alloys with x larger than 0.4 could not be grown.

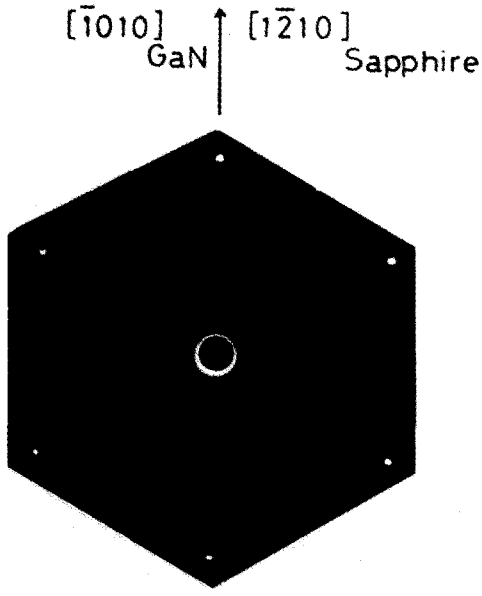

Fig. 4. Back reflection X-ray Laue pattern for GaN grown on (0001) sapphire. The [$\bar{1}$010] direction of the GaN coincides with the [1$\bar{2}$10] direction of the sapphire.

3. Results for GaN

3.1. Surface morphology

Fig. 3 shows scanning electron micrographs of the GaN film grown on a (0001) sapphire substrate with (fig. 3a) and without (fig. 3b) the AlN buffer layer. The former is quite smooth and has no cracks, while the latter shows a rough surface

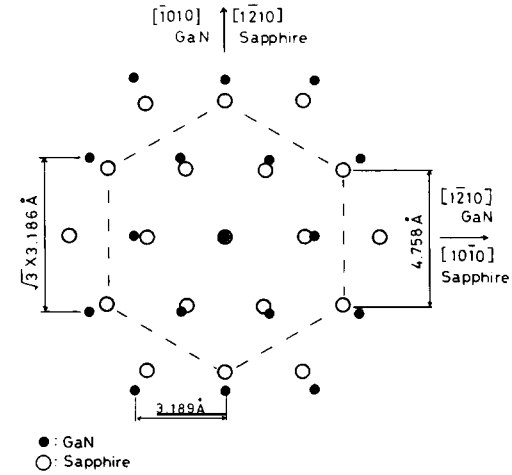

Fig. 5. Schematic illustration of the relation in crystallographic orientation between the (0001) GaN film (●) and the (0001) sapphire substrate (○).

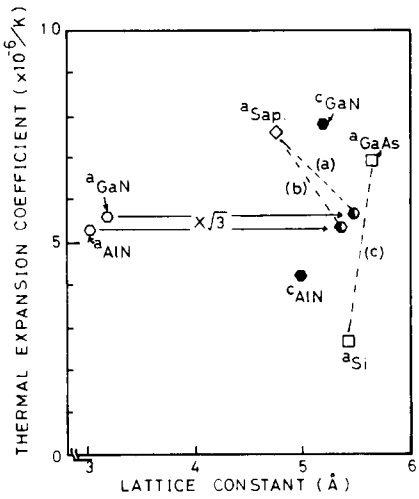

Fig. 6. Differences in lattice constant and thermal expansion coefficient between (a) GaN and sapphire. (b) AlN and sapphire and (c) GaAs and Si. $a_{sap.}$ and $\sqrt{3}\,a_{nitride}$ are taken as the lattice constants.

having hexagonal hillocks. This result shows that the surface morphology of the GaN films can be improved by the predeposition of an AlN layer.

3.2. Relation in the crystallographic orientation between GaN film and sapphire substrate

Fig. 4 is an example of the back reflection X-ray Laue patpattern for a GaN film grown on a (0001) sapphire substrate, showing that the film is aligned so that the $[\bar{1}010]$ direction of GaN is parallel to the $[1\bar{2}10]$ direction of sapphire. This is schematically depicted in fig. 5. According to this relation, the lattice mismatch shown in table 1 expresses the ratio $(\sqrt{3}\,a_{nitride} - a_{sap})/a_{sap}$ in the case of the growth on the (0001) substrate. These relations concerning the lattice mismatch and the difference in thermal expansion coefficient are shown in fig. 6, together with those for GaAs grown on Si. It was also found that the GaN film orients the [0001] axis on the $(11\bar{2}0)$ sapphire substrate.

3.3. Photoluminescence

Photoluminescence (PL) spectra for undoped GaN films are shown in fig. 7-1. The samples are

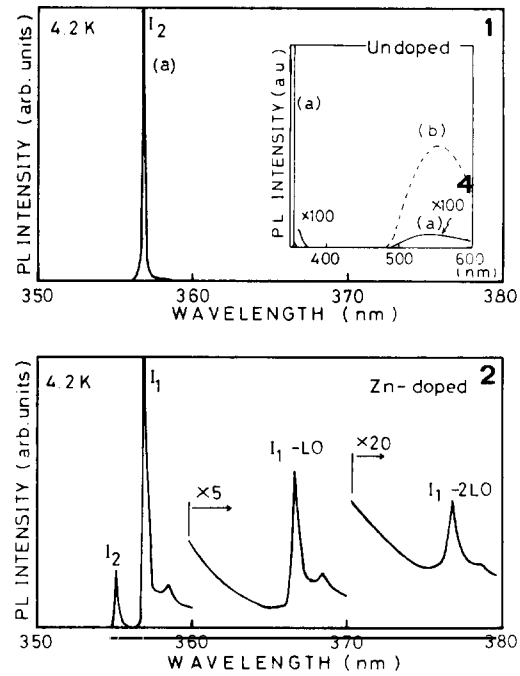

Fig. 7-1. Photoluminescence spectra for undoped GaN films. The samples are the same as those shown in fig. 3. Solid curve (a) is for sample grown with the AlN buffer layer (500 Å thick), and broken curve (b) for the conventional layer. Fig. 7-2. Photoluminescence spectrum for Zn-doped GaN film.

the same as the ones shown in fig. 3. In the GaN film grown with the AlN layer, the I_2 line is very strong and its FWHM is 1.1 meV, which is the

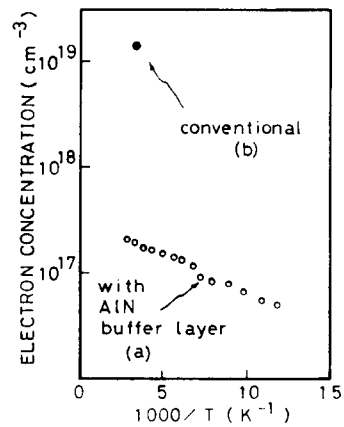

Fig. 8. Electron concentration as a function of reciprocal temperature in GaN film grown (a) with (500 Å thick) and (b) without AlN layer.

best figure up to date in this material. Moreover, a broad band emission in the long wavelength region, which may be due to deep level impurities and/or lattice defects, is scarcely seen. On the other hand, in the conventional film no near band emission is observed; only broad band emission is seen.

In a PL spectrum for a Zn-doped GaN film grown with the AlN layer shown in fig. 7-2, a very strong and sharp I_1 line and its phonon replica clearly appear, while the intensity of the I_2 line is weak compared with the undoped one [6]. This means that Zn behaves as an acceptor and the Zn-doped GaN film grown with the AlN layer is also of high quality.

3.4. Electrical properties

As seen in fig. 8, the electron concentration of the GaN film grown with the AlN layer is two orders of magnitude lower than that of the conventional one. The former electron mobility is about one order of magnitude higher than that of the conventional one, as shown in fig. 9. These data show that the electrical properties are greatly improved by the use of the AlN layer.

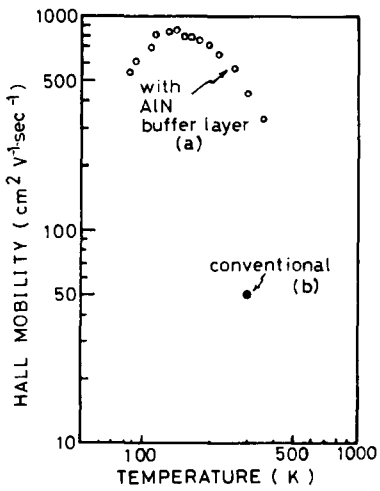

Fig. 9. Temperature dependence of electron Hall mobility of GaN film grown (a) with (500 Å thick) and (b) without AlN layer.

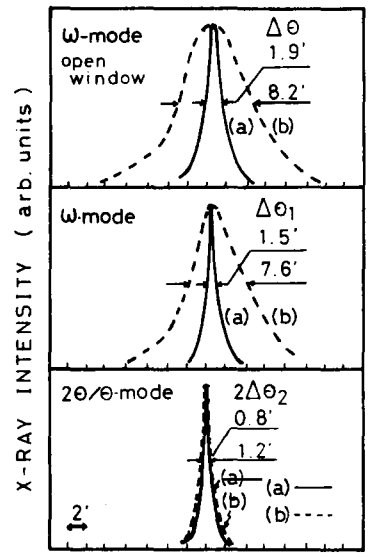

Fig. 10. Double crystal X-ray diffraction profiles obtained from GaN film grown (a) with (500 Å thick) and (b) without AlN layer.

3.5. X-ray diffraction profile

Itoh and Okamoto [7] have shown that if an epitaxial film has a mosaic structure and a variation of lattice spacing, the magnitude of the FWHM of the X-ray diffraction profile depends on the method of measurement. The FWHM $\Delta\theta_1$, which is broadened due to fluctuations in the orientation of the crystallites, is experimentally determined from the rocking curve obtained with the ω-mode using a narrow detector slit. The FWHM $\Delta\theta_2$, which is broadened due to a variation of lattice spacing, can be measured from the diffraction profile by the $2\theta/\theta$-mode with the slit. $\Delta\theta$ is the FWHM for the ω-mode profile obtained with an open detector window, that is, a conventional rocking curve. Therefore, the following superposition rule holds roughly:

$$\Delta\theta = \Delta\theta_1 + \Delta\theta_2. \quad (1)$$

Also, if $\Delta\theta_1$ is much larger than $\Delta\theta_2$, the film is suggested to consist of mosaic crystallites. Fig. 10 shows double crystal X-ray diffraction profiles obtained from the GaN film grown (a) with and (b) without the AlN layer. The magnitudes of $\Delta\theta$ for (a) (solid curve) are much smaller than those

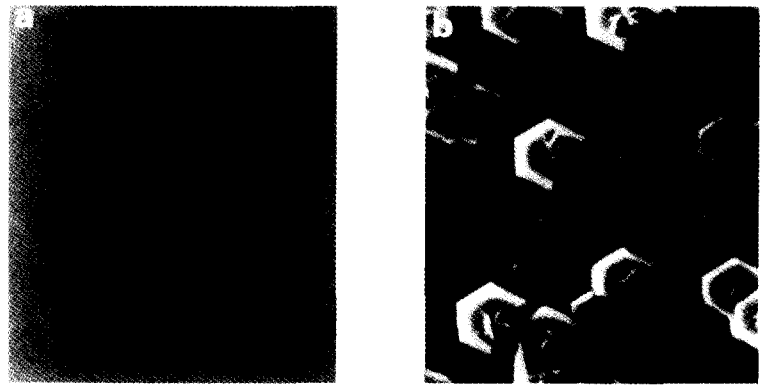

Fig. 11. SEM photographs of $Ga_{0.9}Al_{0.1}N$ film grown on (0001) sapphire (a) with and (b) without AlN layer. The growth time was 60 min. Markers represent 5 μm.

for (b) (dashed curve). The former $\Delta\theta$'s are the narrowest up to date in this material. The variation of the lattice spacing, $\Delta d/d$, was estimated from the magnitude of $\Delta\theta_2$ and the Bragg angle to be on the order of 10^{-4}, which is negligibly small. These results of X-ray studies indicate that by using the AlN layer, the crystalline quality is much improved, although the film is thought to be of mosaic structure, since $\Delta\theta_1$ is much larger than $\Delta\theta_2$.

All these results described in this section show that by the preceding deposition of the AlN layer, the microscopic fluctuation in crystallite orientation and the structural defects originated from this heteroepitaxial growth are significantly reduced and the electrical and optical properties as well as the surface morphology of the GaN film can be remarkably improved.

4. Comparison between GaN and $Ga_{0.9}Al_{0.1}N$

Next, the results for GaN will be compared with those for $Ga_{0.9}Al_{0.1}N$. As seen in fig. 11, a $Ga_{0.9}Al_{0.1}N$ film with a quite smooth surface can be obtained by using the same AlN buffer layer. But, the results of X-ray studies indicate that there is some difference between the GaN film and the alloy film. Fig. 12 shows double crystal X-ray diffraction profiles for the $Ga_{0.9}Al_{0.1}N$ film grown (a) with and (b) without the AlN layer. The magnitudes of $\Delta\theta$ for (a) (solid curve) are much smaller than those for (b) (dashed curve). These results show that the use of the AlN layer is also effective for the alloy growth, although the $Ga_{0.9}Al_{0.1}N$ film consists of mosaic structure ($\Delta\theta_1$ is much larger than $\Delta\theta_2$). However, the magnitudes of $\Delta\theta$ are much larger than those for the GaN film shown in fig. 10, indicating that the crystalline quality deteriorates by the alloying. Moreover, the variation of the lattice spacing was estimated to be on the order of 10^{-3}, which is one order of magnitude larger than that of the GaN film. This

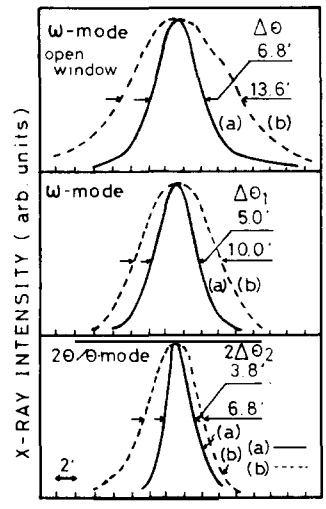

Fig. 12. Double crystal X-ray diffraction profiles for $Ga_{0.9}Al_{0.1}N$ film grown (a) with and (b) without AlN layer.

may be caused by the compositional fluctuation in this alloy, which was previously observed by the present authors in optical absorption spectra [2] and PL spectra [8]. These X-ray results are summarized in table 2. This indicates that in all samples the superposition rule holds, and both the

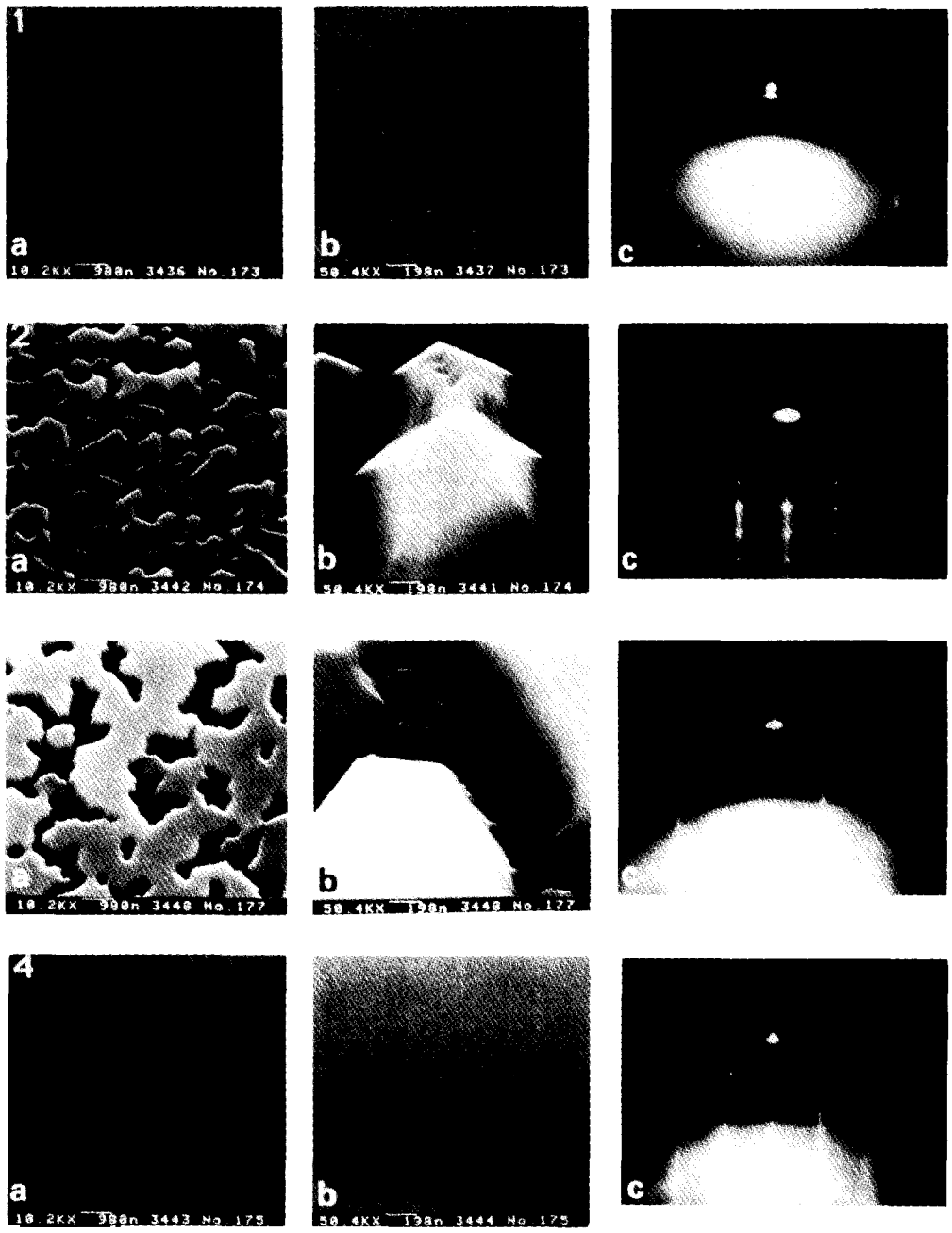

Fig. 13-1. AlN layer deposited at 600 °C for 5 min. Figs. 13-2 to 13-4. GaN film grown at 1000 °C for 5 min (fig. 13-2), 10 min (fig. 13-3) and 60 min (fig. 13-4) on the AlN layer shown in fig. 13-1. Each figure (a) is SEM photograph of the surface, (b) the same as (a) but taken with a high magnification and (c) the corresponding RHEED pattern.

Table 2
FWHMs of X-ray diffraction profiles $\Delta\theta$ and the variation in lattice spacing $\Delta d/d$ of GaN and $Ga_{0.9}Al_{0.1}N$ films

	$\Delta\theta$ (meas.) (arc min)	$\Delta\theta_1$ (meas.) (arc min)	$\Delta\theta_2$ (meas.) (arc min)	$\Delta d/d$ (estimated)
GaN				
With AlN buffer layer	1.9	1.5	0.4	3.7×10^{-4}
Conventional	8.2	7.6	0.6	5.6×10^{-4}
$Ga_{0.9}Al_{0.1}N$				
With AlN buffer layer	6.4	4.5	1.9	1.8×10^{-3} a)
Conventional	13.6	10.2	3.4	3.2×10^{-3} a)

a) Due to compositional fluctuation [2,8].

GaN and the $Ga_{0.9}Al_{0.1}N$ films are composed of many mosaic crystallites. The alloy film includes compositional fluctuation, which differs in quality from the GaN film.

5. Model for the mode of growth

In spite of these X-ray results, it is clear that the crystalline quality as well as the surface morphology of both the GaN and the alloy films can be remarkably improved by the predeposition of an AlN layer.

In order to clarify the role of the AlN layer, every stage of GaN growth was studied by SEM and RHEED.

Fig. 13 shows the changes in surface morphology and the corresponding RHEED pattern of the same part during the growth. Fig. 13-1 was obtained for the predeposited AlN layer whose thickness was about 500 Å. Figs. 13-2 to 13.4 were obtained for the GaN film successively grown

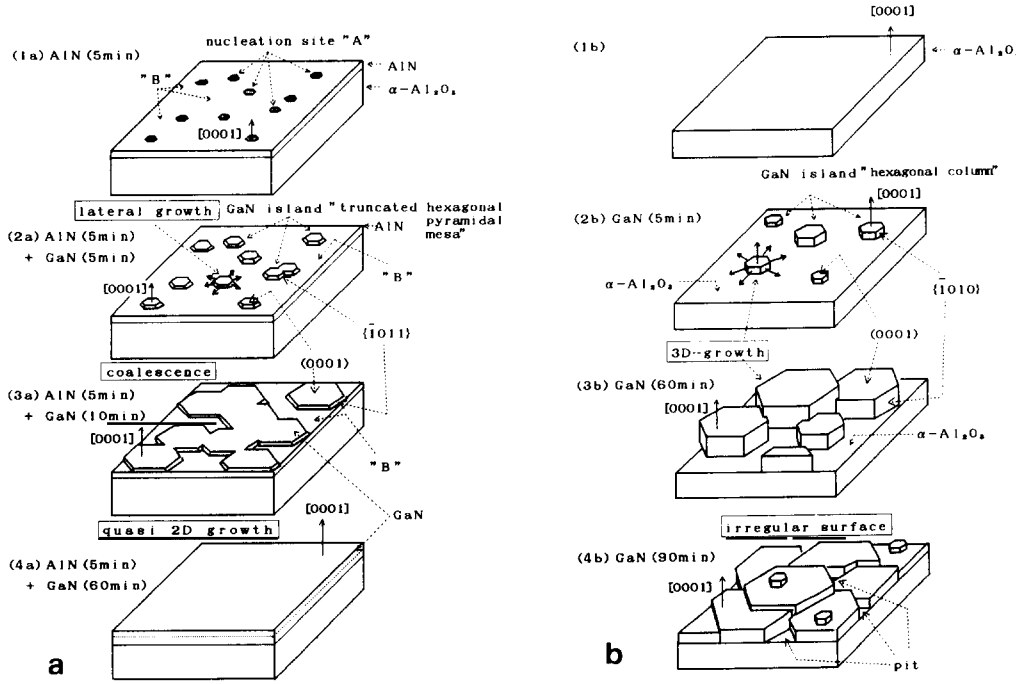

Fig. 14. Growth model for GaN film on (0001) sapphire substrate (a) with and (b) without AlN layer.

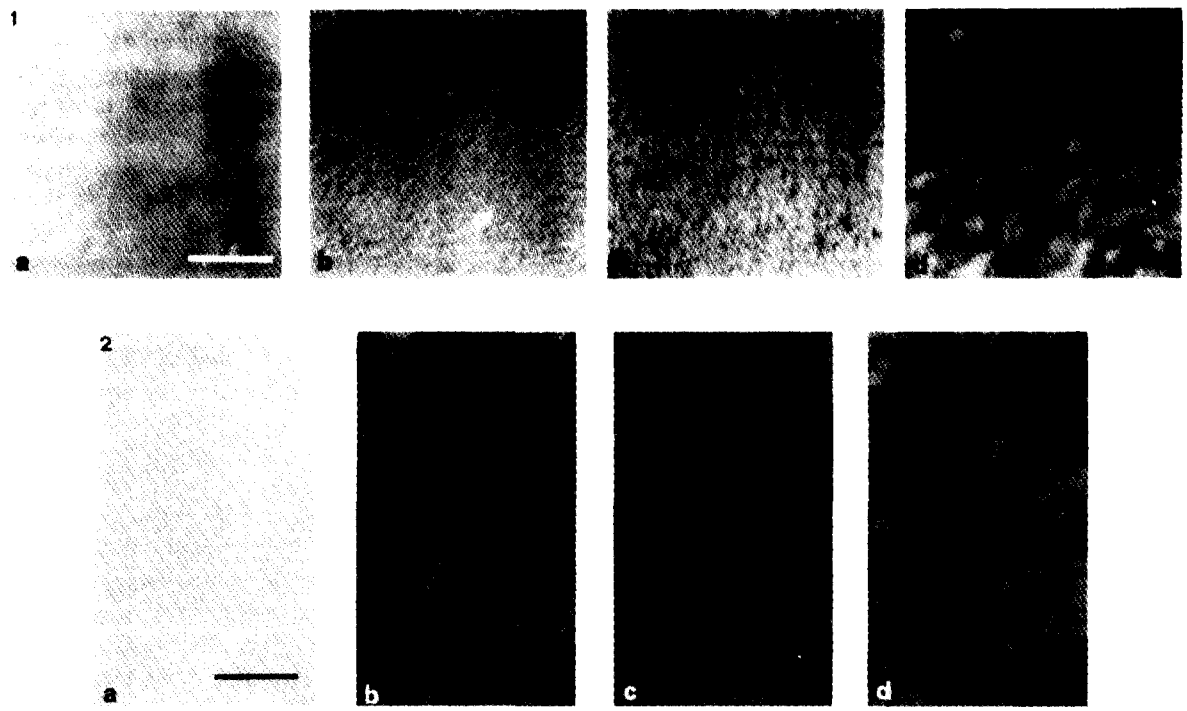

Fig. 15-1. SEM images of AlN layer deposited at (a) 600 ° C, (b) 700 ° C, (c) 900 ° C and (d) 1000 ° C; marker represents 0.3 μm. Fig. 15-2. Differential interference contrast micrographs of GaN film successively grown at 1000 ° C on each substrate covered with AlN layer as shown in fig. 15-1; marker represents 50 μm.

with different growth times on the AlN layer. In each figure, (a) is a SEM photograph of the surface, (b) is the same as (a) but was taken with a high magnification and (c) is the corresponding RHEED pattern. Fig. 13-1 a shows a uniform featureless structure. But in fig. 13-1b, one observes something like fine particles of several tens of Å, which seem to be buried in the featureless structure. The corresponding RHEED pattern (fig. 13-1c) shows somewhat diffuse spots together with a halo-pattern in agreement with the SEM result (figs. 13-1a and 13-1b).

Therefore, this AlN buffer layer is thought to consist of both fine crystallites and an amorphous-like structure. After 5 min of growth, as seen in figs. 13-2a and 13-2b, many truncated hexagonal pyramidal mesas are formed. Successively, a two-dimensional lateral growth proceeds favorably for a certain period of the growth time (figs. 13-3a and 13-3b). This clearly indicates that quasi-lateral growth dominates at a certain thickness of the GaN film. Finally, the whole area of the substrate is covered by GaN film with a flat surface as seen in figs. 13-4a and 13-4b.

The RHEED pattern (fig. 13-2c) after 5 min of growth is spotty, indicating that the GaN islands are three-dimensional. After this, it becomes streaky, indicating that the surface is more flattened (figs. 13-3c and 13-4c).

On the other hand, in the case of direct growth, as shown in fig. 3b, the height of a hexagonal GaN island was proportional to the side at all growth times, indicating that three-dimensional island growth dominates.

On the basis of these results, we propose a model, shown in fig. 14, which can explain the difference in the mode of growth between the two cases.

In the case of the GaN film grown with the AlN layer, under optimum conditions, many AlN crystallites (mode "A"), which are shown by shadowed spots in fig. 14-1a, may be formed

together with an amorphous-like structure. These fine crystallites were found to have the [0001] axis parallel to that of the sapphire and may act as a nucleation center for the following growth of a GaN island, which is not a column, but a truncated pyramidal mesa, as shown in figs. 13-2a and 14-2a. In further growth, the lateral growth and the coalescence of GaN islands are seen (figs. 13-3a and 14-3a). These may be caused by the decrease in interfacial free energy between the GaN island and the amorphous like AlN layer (mode "B").

On the other hand, in the case of the conventional film (fig. 3b), many hexagonal GaN columns with different sizes and heights are formed, as depicted in fig. 14-2b. They grow three-dimensionally (figs. 14-2b and 14-3b), resulting in a rough surface, and many pits at their boundaries, as shown in fig. 14-4b.

The optimum thickness of the predeposited AlN layer was found to be around 500 Å. If it was too thick (for example, 1500 Å), the GaN film became polycrystalline with a rough surface.

Fig. 15-1 shows SEM images of the predeposited AlN layer at different temperatures, and fig. 15-2 shows differential interference contrast micrographs of the GaN film successively grown at 1000 °C on each substrate covered with the AlN layer. As seen in fig. 15, when the deposition temperature of the AlN layer is higher than 600 °C, its surface become rough and the successively grown GaN film became polycrystalline.

Fig. 16 shows the variation of FWHM $\Delta\theta$ of the X-ray rocking curve for the GaN film grown on the substrate covered with the AlN layer, which was predeposited at different temperatures. This shows that the FWHM of the X-ray rocking curve for the GaN film increases suddenly at a certain temperature higher than 600 °C, at which the AlN layer was deposited. These results indicate that the higher the AlN deposition temperature is, the rougher the GaN film becomes.

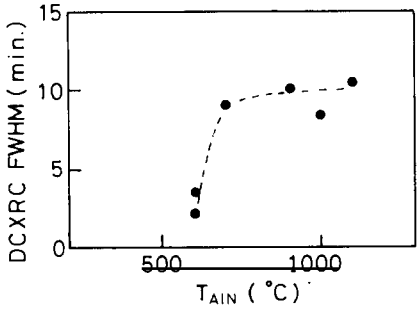

Fig. 16. Variation of FWHM $\Delta\theta$ of X-ray rocking curve for GaN film grown at 1000 °C on AlN layer, which was predeposited at different temperatures.

Therefore, both the thickness and the deposition temperature of the AlN layer were found to be optimal as a buffer layer to convey the information of the substrate, such as the crystallographic orientation, and to relax the strain in this heteroepitaxial growth.

Finally, in order to study the effect of density of the step as a nucleation center, offset-angle substrates were used in conventional MOVPE for comparison, since they are thought to have more nucleation sites than the just-cut substrate. The result showed that, contrary to the growth on the just-cut substrate (cf. figs. 3b and 14-3b), the whole area of the off-angle substrate could be covered by GaN in the growth of 60 min. However, the surface was not specular, but extremely rough. Moreover, the X-ray diffraction profiles were much broader and the PL spectra were much weaker than those of the film grown with the AlN layer. This indicates that the role of the AlN buffer layer cannot be ascribed to the increase in the nucleation site density alone.

6. Summary

GaN and $Ga_{1-x}Al_xN$ ($0 < x \leqq 0.4$) films were epitaxially grown on a (0001) sapphire substrate by MOVPE. By using the thin AlN buffer layer, the surface morphology and the thickness uniformity as well as the electrical and optical properties of these films were remarkably improved. The microscopic fluctuation in crystallite orientation in these films could be considerably reduced, especially in the GaN film. In contrast to the GaN film, $Ga_{1-x}Al_xN$ alloy films include a compositional fluctuation, which caused the variation of the lattice spacing. The optimal thickness and the deposition temperature of the AlN buffer layer were found to be from 500 to 1000 Å and around

600 °C, respectively. The essential role of the AlN buffer layer is thought to be the supply of nucleation centers having the same orientation as the substrate and the promotion of lateral growth of the film due to the decrease in interfacial free energy between the film and the substrate.

Acknowledgments

The authors would like to thank Professor N. Itoh, University of Osaka Prefecture, for valuable discussions concerning the analysis of X-ray diffraction profiles, and also Messrs. N. Okazaki and K. Manabe, Toyoda Gosei Co. Ltd., for their help throughout these experiments. This paper was in part supported by the Scientific Research Grant-in-Aid for Specific Project Research on "Alloy Semiconductor Physics and Electronics" from the Ministry of Education, Science and Culture.

References

[1] I. Akasaki, H. Amano, N. Sawaki, M. Hashimoto, Y. Ohki and Y. Toyoda, Japan Ann. Rev. Electron Computers Telecommun. 19 (1986) 295.
[2] Y. Koide, H. Ito, M.R.H. Khan, K. Hiramatsu and I. Akasaki, J. Appl. Phys. 61 (1987) 4540.
[3] H. Amano, N. Sawaki, I. Akasaki and Y. Toyoda, Appl. Phys. Letters 48 (1986) 353.
[4] I. Akasaki, H. Amano, K. Hiramatsu and N. Sawaki, in: Proc. 14th Intern. Symp. on GaAs and Related Compounds, Heraklion, Crete, 1987, Inst. Phys. Conf. Ser. 91, Eds. A. Christou and H.S. Rupprecht (Inst. Phys., London–Bristol, 1988) p. 633.
[5] Y. Koide, H. Ito, N. Sawaki, I. Akasaki and M. Hashimoto, J. Electrochem. Soc. 133 (1986) 1956.
[6] H. Amano, K. Hiramatsu, M. Kito, N. Sawaki and I. Akasaki, J. Crystal Growth 93 (1988) 79.
[7] N. Itoh and K. Okamoto, J. Appl. Phys. 63 (1988) 1486.
[8] M.R.H. Khan, Y. Koide, N. Sawaki and I. Akasaki, Solid State Commun. 60 (1986) 509.